



Unraveling the effects of temperature on mass transfer and microbiology in thermophilic and extreme thermophilic trickle bed biomethanation reactors

Mads Ujarak Sieborg^a, Nicolaas Engelbrecht^a, Abhijeet Singh^{b,c}, Anna Schnürer^c, Lars Ditlev Mørck Ottosen^{a,d}, Michael Vedel Wegener Kofoed^{a,d,*}

^a Department of Biological and Chemical Engineering, Aarhus University, Gustav Wieds Vej 10C, DK-8000 Aarhus C., Denmark

^b Palaeobiology, Department of Earth Sciences, Uppsala University, Uppsala 752 36, Sweden

^c Department of Molecular Sciences, Uppsala BioCenter, Swedish University of Agricultural Sciences, Box 7015, SE-750 07 Uppsala, Sweden

^d The Novo Nordisk Foundation CO2 Research Center (CORC), Aarhus University, Gustav Wieds Vej 10C, DK-8000 Aarhus C., Denmark

ARTICLE INFO

Keywords:

Biomethanation
Trickle bed reactors
Reactor temperature
H₂ gas-liquid mass transfer
Extreme-thermophilic
Methanogens

ABSTRACT

Numerous initiatives are currently being initiated to substitute fossil fuels with renewable alternatives. Biomethanation is one of these emerging initiatives that presents a novel platform for valorizing carbon dioxide (CO₂) to produce methane (CH₄) by utilizing renewable hydrogen (H₂). Process temperature is a critical factor affecting CH₄ productivity and selectivity, which previously has been ascribed solely to either biological or physicochemical changes. For the first time, this study demonstrated the temperatures effect on the intertwined biological, physicochemical, and process-engineering factors in novel trickle bed reactors (TBR). It was demonstrated that CH₄ selectivity was enhanced by gradually ramping temperature from 55 °C to 70 °C resulting in 62 % reduction in acetate levels. However, further temperature increases > 70 °C deteriorated biocatalytic activity, for which the activity completely stopped at 85 °C. A comparative analysis of a thermophilic TBR (50 °C) and extreme-thermophilic TBR (70 °C) demonstrated 24.6 % improvement in CH₄ productivity at 70 °C. Hereto, the effect of temperature on the H₂ gas-liquid mass transfer rate was modeled, which indicated an increasing trend in mass transfer up to 65.4 °C, whereafter the driving force became too impaired by reduced H₂ solubilities and elevated moisture content in the gas phase. A contribution of only 6.4 % enhancement in the CH₄ productivity from 50 °C to 70 °C could be attributed to the increased H₂ mass transfer rate, which made the temperature effect on the biocatalyst the most pronounced factor for the enhanced process performance and selectivity. Hereto, *Methanothermobacter* was identified as the dominant CO₂-fixing biocatalyst, and *Acetomicrobiaceae* as the major bacterial family correlating with acetate accumulation.

1. Introduction

In the past decades, the impending climate crisis has generated momentum for expanding renewable energy production. In 2015, many countries signed the Paris Agreement, which is a framework committed to addressing climate change by approaching net zero in anthropogenic carbon dioxide (CO₂) emissions [1]. Achieving carbon neutrality by 2050 has been envisioned through energy system transformation towards heavy electrification with a shift in the power mix toward renewable sources. Accordingly, the share of renewable energy is projected to expand up to 38 % by 2027, with predominately wind and solar photovoltaic expansion accounting for 80 % of the renewable energy [2]. However, as renewable energy paves the way for decarbonization,

its stochastic nature puts further strains on the electricity grid. Additionally, the 'hard-to-abate' sectors including long-haul transport, chemical production, high-temperature industrial heating (>400 °C), and iron and steel production cannot be fully electrified and rely heavily on carbon-based energy carriers with a high volumetric energy density. Thus, integrating power-to-X technologies such as biomethanation that exploits H₂ from renewable power to reduce CO₂ to methane (CH₄) as an energy carrier is imperative for decarbonization. Biomethanation enables reaching the grid-scale energy demands with its long charge hold cycles and high storage capacities, which are required to balance the seasonal fluctuation and enable a bidirectional coupling between the electricity and gas sectors.

Biomethanation is a catalyzed process relying on the autotrophic

* Corresponding author at: Department of Biological and Chemical Engineering, Aarhus University, Gustav Wieds Vej 10C, DK-8000 Aarhus C., Denmark.

E-mail address: Mvk@bce.au.dk (M.V.W. Kofoed).

<https://doi.org/10.1016/j.cej.2025.161179>

Received 10 October 2024; Received in revised form 26 February 2025; Accepted 1 March 2025

Available online 2 March 2025

1385-8947/© 2025 The Author(s). Published by Elsevier B.V. This is an open access article under the CC BY license (<http://creativecommons.org/licenses/by/4.0/>).

catabolism of hydrogenotrophic methanogens (HM), which characterizes the final stage of anaerobic digestion. However, the biomethanation process can also be performed separately in an *ex situ* reactor, where the methanogenic conversion step is functionalized in a system for selective high-rate CH₄ production [3]. The main challenges for these *ex situ* biomethanation systems include exothermic heat, H₂ competition with *Bacteria* with acetogenic functions, and the low H₂ gas-liquid mass transfer rate, where the latter has been reported several times as the limiting factor hindering the availability of H₂ to the HM [4–6]. Among the different reactor designs, the trickle bed reactor (TBR) has been demonstrated to facilitate high H₂ mass transfer rates with low specific energy requirements by achieving CH₄ productivities of up to 15.4 L_{CH₄}L_R⁻¹d⁻¹ [7]. However, this productivity is highly dependent on the operational conditions, among which process temperature is a key regulating factor.

Process temperature plays an important role in regulating metabolic processes while having an essential effect on the physicochemical processes. From a thermodynamic point-of-view, the biochemical reaction kinetics proceed much faster at higher temperatures because of the increased rate of the enzymatic reactions until the point of denaturation [8]. Elevating the temperature induces higher maintenance energy requirements (energy flux from catabolic reactions to maintain cellular activity) [9], which stimulates a higher CH₄ productivity to balance the energy requirements [10]. Accordingly, the CH₄ production rate for biomethanation is often demonstrated to be higher in thermophilic bioreactors compared to their mesophilic homologues [11,12]. For an H₂ mass transfer limited process such as biomethanation, achieving higher CH₄ productivities at higher temperatures has been attributed to the lower concentration of dissolved H₂, due to elevated biological reaction kinetics, which improves the driving force for H₂ gas–liquid mass transfer [13]. Additionally, the process temperature affects the gas–liquid mass transfer in several physicochemical aspects, including the solubility of the gases, the diffusion rate, the liquid viscosity, and the gas flow rate [14,15]. An analysis of abiotic data by Jensen et al. suggested a 33 % improvement of the H₂ gas–liquid mass transfer rate when increasing the temperature from 35 °C to 65 °C, as the diffusion coefficient for H₂ would increase by 85 %, whereas the solubility of H₂ was only reduced by 2–4 % [14].

For the biomethanation process, the CH₄ selectivity is mainly challenged by the substrate competition between the homoacetogenic conversion of H₂ and CO₂ to acetate, especially as the competition between *Archaea* and *Bacteria* intensifies at lower temperatures [16]. In contrast, the microbial community typically shows a lower diversity at thermophilic compared to mesophilic biomethanation [17], and even less diverse at extreme-thermophilic temperatures [18], as the higher temperatures selectively promote CH₄ production. Moreover, a study by Ahring et al. reported that the activity of acetoclastic methanogens and butyrate-, formate-, and glucose-degrading *Bacteria* was significantly reduced when increasing the temperature of an anaerobic digester operating with manure from 55 °C to 65 °C, whereas the HM demonstrated an enhanced activity [19]. Likewise, a lower accumulation of volatile fatty acids (VFA) has been reported for thermophilic syngas biomethanation compared to mesophilic conditions [20] and when increasing the temperature from 55 °C to 65 °C [21].

In general, the factors affected by temperature in biomethanation are multitudinous, which makes the overall effect of the process temperature challenging to predict. The temperature affects the microbial biocatalyst by regulating the microbial community structure, kinetics, and energetic yield of metabolic pathways, while also affecting the physicochemical parameters of mass transfer, moisture content in the gas phase, and many more. Hence, this study aimed to shed new light on the influence of operational temperature on these individual parameters to maximize the efficiency and selectivity of the biomethanation process with mixed cultures. Process performance, stability, and microbial development were evaluated by temperature ramp-up in a long-term operated TBR with declining CH₄ productivity at >70 °C. This further leads to a comparative study presented herein of two trickle bed

reactors operated at thermophilic (50 °C) and extreme-thermophilic (70 °C) conditions for biomethanation. Based on the temperature range of mesophilic to extreme-thermophilic metabolic activity, the relative H₂ gas–liquid mass transfer was modeled to quantify the individual physicochemical and microbial contributions to the performance improvement at higher temperatures.

2. Materials and methods

2.1. Configurations of trickle bed reactors

Two custom-built TBRs were installed at the Foulum biogas plant (Aarhus University, Denmark). One TBR was built of stainless steel to accommodate higher temperatures (R1A and R2B), and another TBR was manufactured from polypropylene (R2A). Only one reactor (R1A) was operated in trial 1, followed by the operation of both reactors (R2A and R2B) in trial 2. Both TBRs were designed with an active working volume of 9.09 L, constituting a height-to-diameter ratio of 10 (height: 1.05 m and inner diameter: 0.105 m). Crushed expanded clay aggregates (Filtralite NC 2–10, Leca, Denmark) were selected as carrier material for the bioreactors due to their high dynamic liquid hold-up and specific surface area. The TBRs contained 2.25 kg each of carrier material, characterized by a porous surface structure with a void fraction of 55 %, a particle size range of 2–10 mm, and a bulk density of 250 ± 50 kg m⁻³. The reactor temperatures were maintained with tracing cable (6 m coiled cable at 10 W m⁻¹ rating) (RS, Denmark) and regulated with ON/OFF switches (RS, Denmark). Thermowells in the middle of the reactors housed PT100 temperature probes (Correge, France) as input to the temperature controllers. The pressure was continuously monitored with pressure sensors (GEMS Sensors & Controls, USA). The internal concentration gradient of H₂ was measured with H₂ microsensors (Unisense, Denmark) mounted in the bottom, middle, and top sections and monitored with the Unisense Logger program with data sampling every 1 min, for which the method has been previously validated in biomethanation systems [22]. However, these microsensors were only used for operation at <60 °C, above which the gas concentration was monitored solely with gas chromatography (GC). The individual substrate gas flows of raw biogas and electrolyzer H₂ were continuously supplied with mass flow controllers (SLA5850, Brooks Instruments, USA) to a manifold for mixing before being supplied to the TBRs in a counter-flow configuration. The H₂ was produced by an anion exchange membrane water electrolysis system (EL 1.0, Enapter, Germany) and pressurized to 35 bar_g. Raw biogas was supplied from an agricultural-based biogas plant with a total capacity of 4 700 m³ divided into a primary digester (1 200 m³) and a secondary digester (3 500 m³) (Foulum, Denmark). The raw biogas required for the TBR was compressed to 3 bar_g in a 500 L compressor tank to supply the mass flow controllers. The nutrient media for microbial growth was delivered with cone-spray nozzles (1 mm diameter) and recirculated daily from individual reservoirs containing 1 L solution. Individual peristaltic pumps were used for R2A (LabN1 pump, Shenchen) and for R1A and R2B (WT3000-1JA Micro Gear, Longerpump, China) to avoid mixing the microbial cultures. The flow rates of the product gas streams were monitored with drum flow meters (Ritter, instrument no: TG-5/0.5, Germany) before the product gas was sent to an intermediate gas storage facility at the biogas plant, which had a capacity of 1 200 m³. A detailed process flow diagram is shown in the diagram of Fig. 1.

2.2. Bioreactor operation

Trial 1 (R1A) was operated for an extended period of 594 days in total. Hereof, the initial 221 days constituted two other studies [22,23], while day 222 to 594 were included in this study (total of 372 days). Day 222 of the reactor operation has been marked as day 1 for trial 1. The commencement of trial 2 (R2A and R2B) was conducted subsequently to trial 1 (R1A). The continuous gas supply of raw biogas and electrolyzer

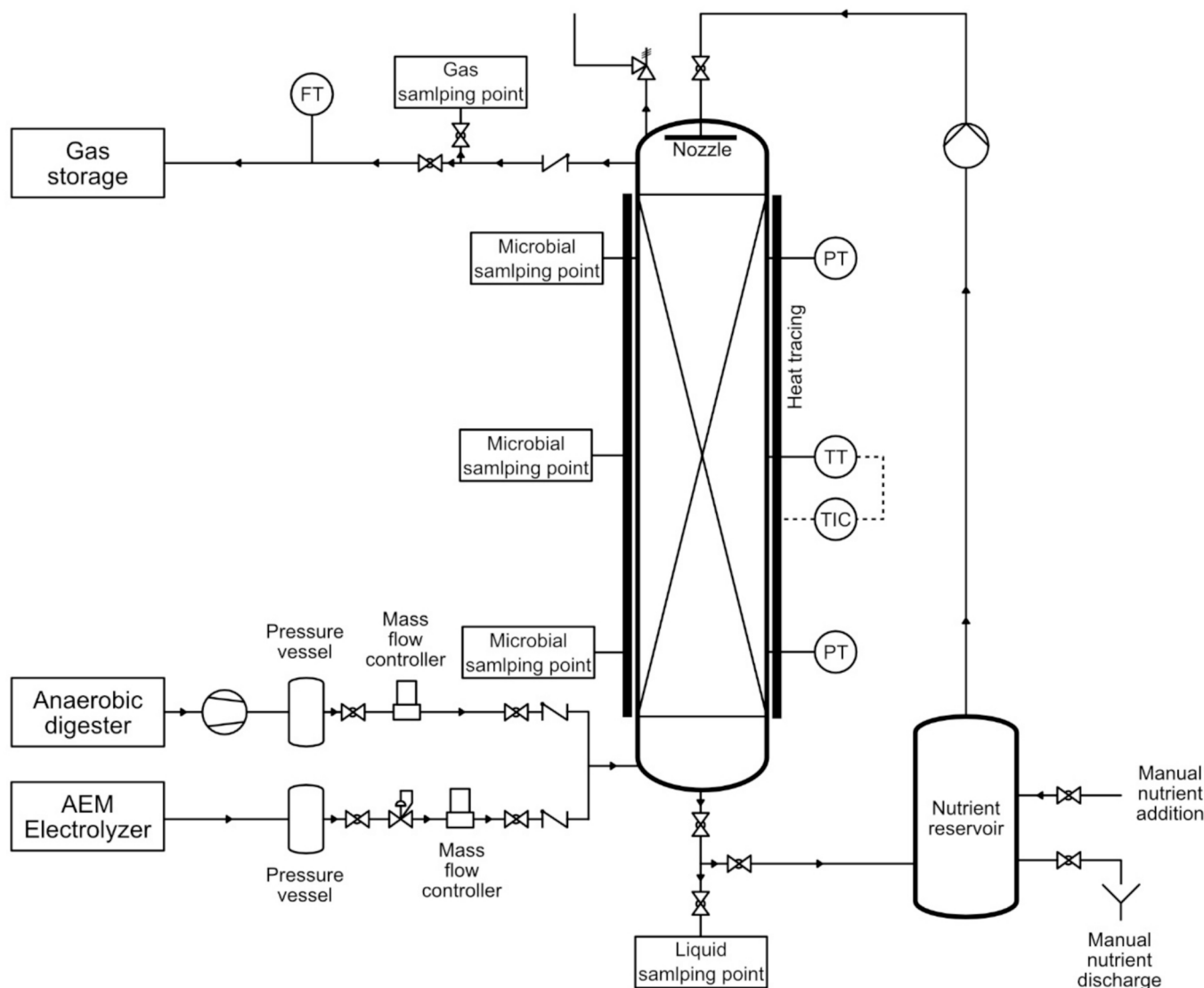


Fig. 1. Overview of the process flow diagram of the trickle bed bioreactor (R1A, R2A, and R2B), the configurations, the upstream H₂ and biogas infrastructure, and the downstream gas storage.

H₂ was administered in trial 1 with a constant load of 42.84 L_{H₂} L_R⁻¹ d⁻¹ H₂ and 26.63 L_{biogas} L_R⁻¹ d⁻¹ raw biogas (12.09 L_{CO₂} L_R⁻¹ d⁻¹ CO₂) and with an initial gas load in trial 2 of 13.3 L_{H₂} L_R⁻¹ d⁻¹ H₂ and 7.1 L_{biogas} L_R⁻¹ d⁻¹ raw biogas (3.25 L_{CO₂} L_R⁻¹ d⁻¹ CO₂). In trial 2, the substrate feed gases were increased proportionally, corresponding to 3.25 L_{CO₂} L_R⁻¹ d⁻¹ of CO₂ load when each of the TBRs demonstrated 3 consecutive days with CH₄ concentrations above 95 % in the product gas. This conversion-dependent ramping created individual ramp events for the thermophilic and extreme-thermophilic biomethanation reactors. The inherent variations in substrate compositions from the biogas plant prompted fluctuations in the composition of the raw biogas during the experimental period. The average composition of raw biogas administered to the TBR during trial 1 was quantified to be 54.3 ± 1.4 % CH₄ and 45.7 ± 1.4 % CO₂ with an H₂S concentration of 1 319.9 ± 138.2 ppm (n = 14). This was used as a setpoint reference for the biogas supply for the respective reactors in this study.

A synthetic nutrient media of essential minerals and buffers was recirculated daily (trickling). The nutrient media was composed of 5 349.1 mg L⁻¹ NH₄Cl, 43.8 mg L⁻¹ EDTA, 61.0 mg L⁻¹ MgCl₂ 6 H₂O, 81.1 mg L⁻¹ FeCl₂ 6 H₂O, 1.2 mg L⁻¹ CoCl₂, 1.3 mg L⁻¹ Na₂MoO₄ 2 H₂O, 1.1 mg L⁻¹ NiCl₂, 23.4 mg L⁻¹ Na₂S, 5 000 mg L⁻¹ K₂HPO₄, 1 000 mg L⁻¹ KH₂PO₄, and 500 mg L⁻¹ Na₂CO₃. Trickling was limited to a daily periodic

trickling with varying flow rates to reduce channeling by the procedure: 70.1 L_{liquid} L_R⁻¹ d⁻¹ for 1 min followed by 40.2 L_{liquid} L_R⁻¹ d⁻¹ for 5 min and repeated three times. The liquid reservoir constituted a nutrient media volume of 1 L media with an exchange rate of 0.4 L d⁻¹, which was exchanged periodically just before trickling was initiated. The high exchange rate was applied to the system to reach a fast biological stabilization within the microbial communities by limiting the recycling of microbial biomass and enabling microbial structure analyses. The metabolic water produced from the biomethanation reaction was subsequently also removed to avoid nutrient dilution. An overview of the operational conditions for the different TBRs is listed in Table 1.

Trial 1 commenced on day 222 of the total operation period of R1A (day 1 in trial 1). Gradual acidification was a recurring issue [22,23], and the experimental period thus examined different preventive initiatives to alleviate VFA accumulation. Day 1–45 of trial 1 included regular operation to quantify the maximum conversion rate before acidification reduced the stability and conversion rate of R1A. On day 46–69, the trickling liquid was pH regulated to a pH of 7.00 with 0.1 M NaOH before trickling was initiated. On day 70–85, filtering accumulated biomass out of the recirculated media to avoid decay as a source for VFA production was examined. On day 88–106, the effect of removing accumulating VFAs in the TBR was examined by trickling water through

Table 1
Operational conditions for the three different trickle bed reactors used in the study.

Trial no.	Trial 1		Trial 2	
	R1A		R2A	R2B
Temperature	55–85 °C		50 °C	70 °C
Total operation	594 days		50 days	50 days
Experimental period	372 days Continuation (From day 222–594)		50 days	50 days
Substrate gases	Electrolyzer H ₂ Raw biogas		Electrolyzer H ₂ Raw biogas	Electrolyzer H ₂ Raw biogas
Trickling frequency	Daily		Daily	Daily
Trickling rate	70.1 L L ⁻¹ d ⁻¹ for 1 min 40.2 L L ⁻¹ d ⁻¹ for 5 min Repeated three times		70.1 L L ⁻¹ d ⁻¹ for 1 min 40.2 L L ⁻¹ d ⁻¹ for 5 min Repeated three times	70.1 L L ⁻¹ d ⁻¹ for 1 min 40.2 L L ⁻¹ d ⁻¹ for 5 min Repeated three times
Nutrient media	Synthetic		Synthetic	Synthetic
Inoculum source	Decanted digestate		Decanted digestate	Decanted digestate
Carrier material	Crushed expanded clay		Crushed expanded clay	Crushed expanded clay

the TBR for 5 min at 40.2 L_{H₂O} L_R⁻¹ d⁻¹ before the nutrient trickling. On day 114–125, the possibility of microbially converting the VFAs by implementing an intermittent operation pattern with 12 h of reactor shutdown with low H₂ partial pressure was examined [23]. On day 130–170, the effect of applying different phosphate buffers (K₂HPO₄ up to 10 g L⁻¹) in the nutrient media was tested. Finally, the impact of temperature was examined from day 171–372 by a gradual ramp up from 55 °C (day 171–250), 60 °C (day 251–277), 65 °C (day 278–298), 70 °C (day 299–325), 75 °C (day 326–350), 80 °C (day 351–365), and 85 °C (day 366–372).

2.3. Inoculation

The source of inoculum for the TBRs was the liquid fraction of digestate from the thermophilic digester (52 °C, 1200 m³) of the agricultural manure-based biogas plant (Foulum, Denmark). A decanter centrifuge (Type UCD 305-00-02, Westfalia Separator Industry GmbH) was used to obtain the liquid fraction of the digestate. Two different batches of inoculum with slightly different characteristics were extracted (Table A1, supplementary materials), with inoculum 1 for the inoculation of R1A and inoculum 2 for the inoculation of R2A and R2B. The substrate gases of H₂ and CO₂ (raw biogas) were used to create an anaerobic environment before inoculating each of the TBRs. When the anaerobic environment had been established, the inoculum was pumped into the TBRs until the reactor was flooded to ensure complete coverage of carrier materials with the inoculation culture. After flooding, the liquid was recirculated for 5 h at a rate of 46.5 L_{liquid} L_R⁻¹ d⁻¹ for R1A and 70.1 L_{liquid} L_R⁻¹ d⁻¹ for R2A and R2B. After the recirculation was stopped, a total volume of ~0.65 L was retained by the carrier material within each reactor.

2.4. DNA extraction

Samples for microbial analysis were collected from R1A in trial 1 at day 250 (55 °C), 277 (60 °C), 298 (65 °C), 325 (70 °C), 350 (75 °C), 365 (80 °C), 372 (85 °C) and from R2A and R2B in trial 2 at day 0, 2, 5, 8, 11, 15, 20, 23, 27, 30, 34, 37, 40, 43, 46, and 50. The extraction point from the reactors was near the gas inlet (at 12.5 cm reactor height). The microbial material was collected by suspending 1–2 g carriers in 3 mL phosphate buffer (0.05 M K₂HPO₄) followed by a 30 s vortex period at 3 000 RPM to release microbial cells from the carriers before DNA extraction. A 2 mL volume of cell suspension was concentrated by centrifugation at 7 000 g for 10 min followed by dissolving the cell pellet in 300 µL of RNA-free water. DNA was extracted from the concentrated cell suspension using FastDNATM SPIN Kit for soil (MP biomedical, France) in accordance with the manufacturer's protocol, including an

additional cleaning step with guanidine thiocyanate for Illumina sequencing and qPCR [24]. The DNA extractions were conducted in triplicates for samples further processed by qualitative polymerase chain reaction (qPCR) and in singlets for Illumina sequencing.

2.5. 16S rRNA gene amplicon sequencing and analysis

Illumina 16S rRNA gene amplicon sequencing was performed on the samples from R1A, R2A, and R2B. The PCR amplification, purification, and barcoding for Illumina sequencing were performed according to published methods [24], and the sequencing was conducted by SciLifeLab (Sweden) using the MiSeq Illumina (2x300 bp) sequencing platform. A universal primer set of 515F forward primer and 806R reverse primer was used for the amplification to target both the entire microbial community of *Archaea* and *Bacteria* [25].

The 16S rRNA gene amplicon sequencing data were analyzed using the de-multiplexed fastq reads. Cutadapt (v3.5) [26] was used for the adapter and primer removal and quality control (Q-score > 20). On average, 434 886 de-multiplexed fastq paired end reads per sample were obtained, and 125 217 (58 %) were retained after adapter trimming and quality filtering. The quality controlled paired end reads were merged using VSEARCH (v2.21.1) [27], and 121 918 merged reads (merging percentage = 96.3 %) were obtained. Chimeric sequence removal and generation of amplicon sequence variants (ASV) were performed on the merged sequences using package *dada2* (v1.22.0) [28] in RStudio (v2021.09.0 + 351) [29] running R (v4.1.3) [30].

On an average, 99 738 reads per sample were non-chimeric and used to analyze sequence variants, resulting in 1 216 ASVs. Taxonomic annotations of ASVs were performed using the 16S rRNA database formatted for *dada2* with Genome Taxonomy Database taxonomies (v207) [31]. The abundance table, taxonomy table, sample metadata, and phylogenetic tree were merged into a single object and used for visualization and statistical analysis using packages *phyloseq* (v1.38.0) [32], *vegan* (v2.6.2) [33], and *ggplot2* (v3.3.6) [34]. Of 1 219 ASVs, 132 *Archaea* and 1 084 *Bacteria* were taxonomically classified (at kingdom level). The differential abundance analysis was done with package *DESeq2* (v1.34.0) [35]. The de-multiplexed paired end fastq reads were deposited to the SRA at NCBI with the accession number PRJNA1142967.

2.6. Quantitative polymerase chain reaction (qPCR)

The qPCR analyses were performed on the same samples from R1A in trial 1. Primers MBT857F (5'-CGWAGGGAAGCTGTAAAG-3') and MBT1196R (5'-TACCGTCGTCCACTCCTT-3') were used to target *Methanobacteriales* [36]. The qPCR was performed with a QuantStudioTM 5

thermocycler (Applied Biosystems, Thermo Fischer Scientific, USA). Each qPCR reaction comprised 10 μL of qPCR master mix (ORA™ SEE qPCR Green ROX L Mix 2X, HighQu), 3 μL of PCR-graded water, 1 μL of forward primer (10 nM), 1 μL of reverse primer (10 μL) and 3 μL of extracted DNA to a total volume of 20 μL . The standards were quantified in triplicates in the range of gene copies from 10^9 to 10^1 with a 10-fold serial dilution per standard sample and were quantified concurrently with the samples. The qPCR protocol was conducted with an initial temperature of 95 °C for 7 min followed by 40x cycles of 95 °C for 40 sec, 58 °C for 60 sec, and 72 °C for 40 sec. The end of the qPCR assay was marked for quantification of a melt curve analysis of 55 °C to 95 °C with a $\Delta T = 0.15$ °C s^{-1} . The standard curves for the qPCR had a linear correlation for *Methanobacteriales* (gene copies from 10^1 to 10^9) with a r^2 ranging between 0.993 and 0.999. The qPCR efficiency ranged between 86.8 and 98.6 for *Methanobacteriales*.

2.7. Analytical methods

Liquid samples were collected daily before and after the liquid trickling to monitor the pH and VFAs. The pH was analyzed directly with a portable pH meter (Portavo® 902 PH, Knick) to acquire a rapid indication of the reactor stability. The concentrations of VFAs (C2–C6) in the liquid samples were analyzed with a GC (6850, Agilent Technologies, USA) with an HP-INNOVAX column (Agilent Technologies, USA) and a flame ionization detector (FID). The applied carrier gas was helium. The samples were prepared by acidifying 1 mL of liquid sample with 4 mL of 0.3 M oxalic acid. An internal standard of pivalic acid was added to the solution. The liquid fraction was separated from the solid fraction by centrifugation (10 min at 4500 RPM) and filtering (0.45 μm), and then analyzed on the GC. The gas composition of H_2 , CO_2 , CH_4 , N_2 , and O_2 in the product gas was monitored daily with another GC (GC-2014, Shimadzu, Japan) with two sample loops and two columns to separate CO_2 , O_2 , N_2 , and CH_4 with helium as carrier gas (662 Porapak Q column, CS-Chromatographie Service GmbH, Germany) and H_2 using argon as carrier gas (80486-800 ShinCarbon ST packed column, Restek, USA). Each gas constituent was quantified with thermal conductivity detectors.

2.8. Data analysis

The evaluation of process performance was based on multiple performance indicators, including the CH_4 productivity ($\text{NL L}_R^{-1} \text{d}^{-1}$). The raw biogas as substrate included a fraction of CH_4 , which was removed from the mass balance calculation.

$$r_{\text{CH}_4} = F_{\text{out}} \cdot x_{\text{CH}_4, \text{out}} - F_{\text{in}} \cdot x_{\text{CH}_4, \text{in}}$$

here, F_{out} represents the total gas flow rate out of the reactor and normalized to the reactor volume ($\text{L}_{\text{gas}} \text{L}_R^{-1} \text{d}^{-1}$), $x_{\text{CH}_4, \text{out}}$ is the fraction of CH_4 in the outlet flow measured with GC, F_{in} is the inlet flow rate normalized to the reactor volume ($\text{L}_{\text{gas}} \text{L}_R^{-1} \text{d}^{-1}$), and $x_{\text{CH}_4, \text{in}}$ is the fraction of CH_4 in the inlet flow. Another performance parameter is the gas retention time (GRT, min) based on the total gas flow rate into the reactor, F_{in} .

$$\text{GRT} = \frac{V_R}{F_{\text{in}}} \cdot 1440$$

The water vapor fraction in the gas phase is calculated based on the Antoine equation:

$$\log_{10}(p) = A - \frac{B}{C + T}$$

where p is the water vapor pressure (mmHg), T is the temperature (K), and A , B , and C are constants with values of 8.07131, 1730.63, and 233.426, respectively, within the temperature range of 1–100 °C [37]. The Henry constant of H_2 , H_{H_2} , is determined based on a polynomial equation from Kolev, 2011, with experimental data from Grischuk [38],

reported in [39]).

$$H_{\text{H}_2} = -1.543218 \cdot 10^6 + 1.3585 \cdot 10^4 \cdot T + (3.78843 \cdot 10^1) \cdot T^2 + (3.51564 \cdot 10^{-2}) \cdot T^3$$

The volumetric gas–liquid mass transfer rate of H_2 , r_{g-l} , is calculated based on the two-film model:

$$r_{g-l} = k_L \cdot a \cdot (C^* - C_L)$$

where a represents the volumetric gas–liquid interfacial area, k_L is the liquid-side mass transfer coefficient, C_L is the dissolved gas concentration in the bulk liquid, and C^* is the concentration of dissolved gas at the gas–liquid interface, which is related to the H_2 partial pressure, p_{H_2} , and the Henry constant, H_{H_2} [40]:

$$C^* = \frac{p_{\text{H}_2}}{H_{\text{H}_2}}$$

Assuming a stagnant film at the liquid surface, the two-film theory states that the liquid-side mass transfer coefficient is a function of the diffusion coefficient (D_{H_2}) and liquid film thickness (δ_L) [41].

$$k_L = \frac{D_{\text{H}_2}}{\delta_L}$$

where the diffusion coefficient of H_2 in water, D_{H_2} , is temperature dependent and calculated following the correlation of Akgerman and Gainer [42]. A proportional relationship between k_L and D_{H_2} was employed in this study, resulting in the boundary layer thickness, and thus the diffusional length, δ_L , to be independent of the temperature [41].

3. Results and discussion

3.1. VFA management and control strategies for bioreactor selectivity

The thermophilic TBR, R1A, was operated continuously for an extended period of 594 days, which during the initial 221 days encompassed two other studies [22,23]. Trial 1 initiated in the present study commenced on day 222 (day 1 in trial 1). At this point, a stable CH_4 productivity of $10.11 \pm 0.84 \text{ L}_{\text{CH}_4} \text{L}_R^{-1} \text{d}^{-1}$ was achieved during regular operation. However, a recurrent issue of gradual acidification from VFAs ($3169.8 \pm 512.7 \text{ mg L}^{-1}$ VFA with 34 % being acetate) challenged the reactor stability during day 1–45 when efforts were made to increase the CH_4 productivity, as was also the case for the earlier operation [22]. Thus, different preventive initiatives were examined to reduce and alleviate the VFA accumulation and associated problems in R1A between day 1–170, including (1) liquid pH regulation, (2) biomass removal, (3) daily water washout and dilution of VFAs, (4) periodic

Table 2

The effect of VFA control strategies on the acetate and total VFA accumulation in reactor R1A between day 1–170.

VFA control strategy	Tested period [days]	Acetate conc. [mg L^{-1}]	Total VFA conc. [mg L^{-1}]
Baseline operation	45	1088.6 ± 251.9	3169.8 ± 512.7
Liquid pH regulation	23	663.8 ± 256.7	2098.9 ± 522.7
Biomass filtration	15	1116.8 ± 469.0	2829.4 ± 610.8
Daily washout of VFAs	18	864.8 ± 147.7	1974.8 ± 446.0
Periodic low p_{H_2}	11	336.7 ± 84.8	1622.3 ± 341.8
Elevated buffer capacity	40	731.4 ± 300.5	1931.1 ± 733.7

reduction of H_2 partial pressure (p_{H_2}), and (5) elevated buffer capacity (Table 2).

The effect of the VFA control strategies on the acetate and total VFA accumulation demonstrated that the production and accumulation of VFA were a direct response to the continuous operating strategy of the TBR during normal operation. Operating the TBR intermittently for periods without H_2 addition was the most effective VFA control strategy, which enabled the H_2 concentrations to be reduced below the thermodynamic threshold where VFA oxidation, and especially acetate oxidation, became bioenergetically favorable [43]. Although effective in reducing VFA levels, periodic reductions in H_2 partial pressure require periodic pauses in operation. In contrast, liquid pH regulation, daily washout of the VFAs, and elevated buffer capacities were also demonstrated as effective acid management strategies by reducing the acetate concentration by 33.8 %, 37.7 %, and 39.1 %, and the total VFA concentration by 39.0 %, 20.2 %, and 32.8 %, respectively. These strategies maintained a more neutral to alkaline environment for the microbiome, where the *Bacteria* with acetogenic functions have been found less competitive with the HMs [44]. Nevertheless, these approaches of pH control, VFA washout, and increased buffer capacity necessitated more frequent carrier irrigation, which transiently deteriorated the bi-methanation process causing the conversion rates to decline (Fig. A1, supplementary materials). During every initialization of the trickling, the CH_4 productivity temporarily dropped to 46.2 ± 10.9 % of the theoretical maximum CH_4 productivity, and when the trickling was ended, a recovery of 69.8 ± 8.7 % after 10 min and 95.3 ± 7.4 % after 80 min was achieved in terms of CH_4 productivity. This phenomenon

was previously observed [45], and the trickling was therefore limited to once daily. Hence, the lack of a long-term preventive measure to curb VFA accumulation, yet still allow for a continuous bi-methanation process, meant that another approach to those investigated in Table 2 had to be found.

3.2. Temperature as a selective driver for hydrogenotrophic methanogenesis

An alternative approach applied in this study was to limit the VFA accumulation and improve the CH_4 productivity by exploiting reaction temperature, a process parameter entirely decoupled from the liquid trickling. The effect of the temperature was evaluated on the TBRs process performance and microbial community structure (1) when gradually increasing temperature from 55 °C to 85 °C with 5 °C intervals in a long-term enriched TBR (R1A) from day 171–372 and (2) in two freshly inoculated TBRs at 50 °C (R2A) and 70 °C (R2B) for 50 days.

3.2.1. Microbial community structure and dynamics

Analyzing the microbial community structure based on 16S rRNA gene amplicon sequencing revealed a successful enrichment of *Methanothermobacter*, an obligate autotrophic HM from the order *Methanobacteriales*, which dominated the microbial composition of R1A, R2A, and R2B at the applied temperatures from 50 °C to 85 °C (Fig. 2). The genus *Methanothermobacter* has been consistently reported to be selectively enriched from mixed cultures in numerous thermophilic TBR studies [11,46]. This recognition has prompted pure culture

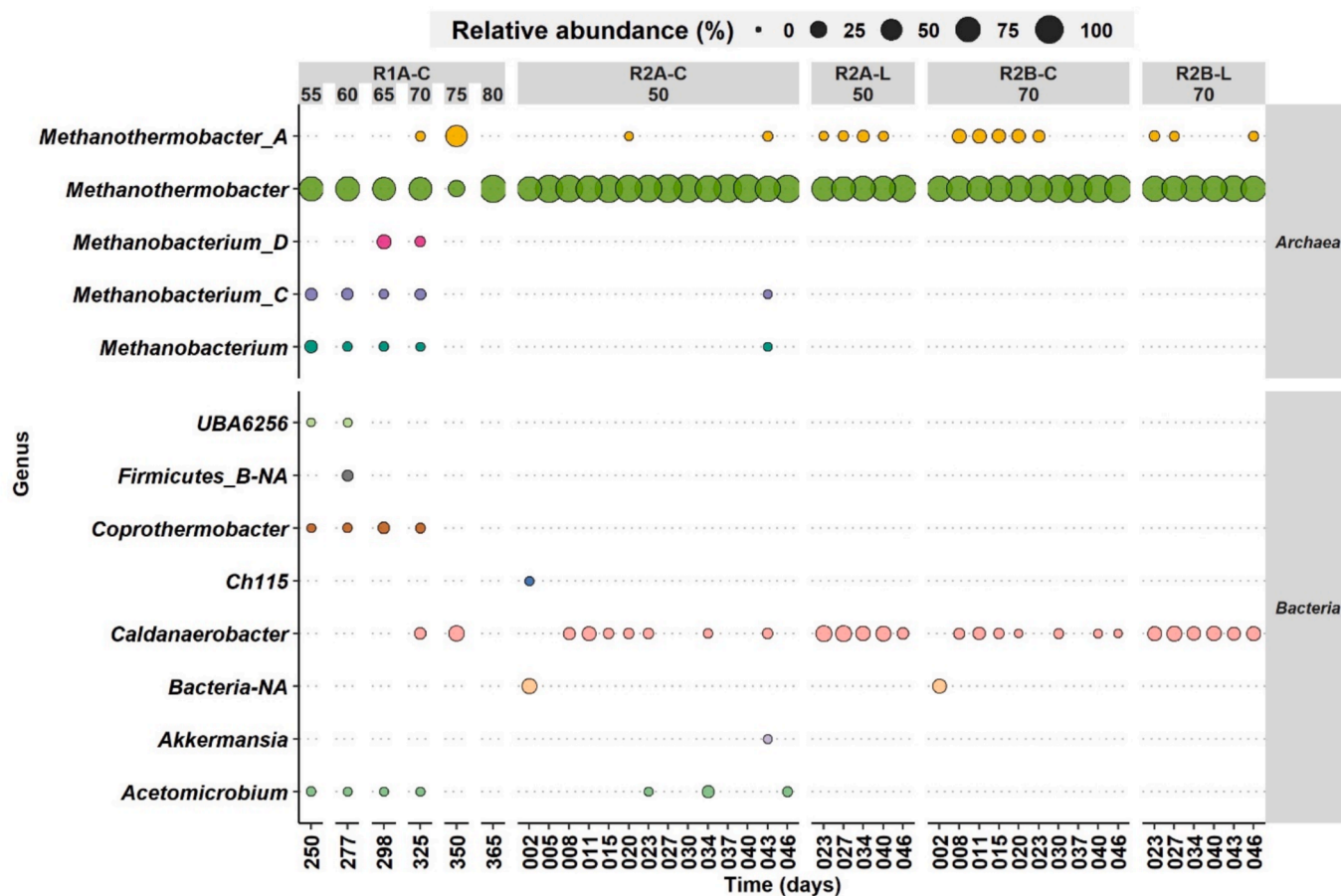


Fig. 2. Bubble plot of the relative abundance (>2 %, depicted by size) of the total archaeal and bacterial community at the genus level in carriers (–C) and process liquid (–L) of the temperature-ramped reactor (R1A), the thermophilic reactor (R2A), and the extreme-thermophilic reactor (R2B). Sampling in reactor R1A was based on each 5 °C increment step in the gradual ramp of temperature from 55 °C to 80 °C, and sampling in reactor R2A and R2B was performed with an interval of 3–4 days throughout the operational period.

biomethanation with *Methanothermobacter* as the biocatalyst candidate in TBRs [47], and industrial scale utilization in biomethanation CSTRs [48]. *Methanothermobacter* accounted for < 4 % of the microbial abundance in the inoculum for R2A and R2B (Fig. A2, supplementary materials), and rapidly increased in abundance in the TBRs (Fig. 2). Interestingly, the analysis also identified various other HMs, such as the genus *Methanobacterium*, within the order *Methanobacteriales* in R1A, regardless of the extended period of operation since inoculation. *Methanobacterium* was mainly represented in R1A at lower temperatures followed by a decline in abundance with increasing temperatures, which was distinctly demonstrated at >70 °C.

The bacterial community in the TBRs constituted only a minor fraction of the entire microbial community. Nevertheless, the role of the bacterial community was still of importance due to its capability to both cause instability by VFA production and/or in contrast ensure stable operation by nutrient recycling and consuming accumulating acids, metabolites, and biomass [23]. However, the high abundance of *Archaea* rendered the investigation of the bacterial community challenging with the applied method. Thus, the archaeal community was filtered out to examine the effect of temperature on the bacterial community only (Fig. 3 and supplementary material, A3 and A4).

The composition of the bacterial community was at the genus level primarily represented by *Acetomicrobium*, *Caldanaerobacter*, and *Coprothermobacter* in all three TBRs. *Coprothermobacter* and *Caldanaerobacter* have previously been identified as core functional *Bacteria* in thermophilic biomethanation [18] with a syntrophic relationship to the main biocatalyst *Methanothermobacter* [49]. Meanwhile, *Acetomicrobium* has been identified in multiple biomethanation studies and has often been reported to be promoted by acidic conditions [22,50–52]. The proliferation of many of the *Bacteria*, such as *Coprothermobacter* and *Acetomicrobium*, subsided at >70 °C in R1A during the gradual temperature ramp-up, whereas *Caldanaerobacter* had a higher relative abundance at 70–75 °C. The ASVs classified as *Caldanaerobacter*, *Coprothermobacter*, and *Acetomicrobium* showed high similarity with the species *Caldanaerobacter subterraneus*, *Coprothermobacter proteolyticus*, and *Acetomicrobium flavidum*, respectively. Previous characteristics demonstrated that *C. subterraneus* exhibits temperature tolerance with a temperature optimum of 65 °C and with a growth rate almost double at 70 °C as compared to at 50 °C [53]. In contrast, *C. proteolyticus* has been reported with a temperature optimum of 63 °C and has demonstrated difficulty adapting to elevated temperatures of 70 °C [54,55]. Accordingly, the relative abundance of *Coprothermobacter* was lower at 70 °C



Fig. 3. Bubble plot of the relative abundance (>2%, depicted by size) of the bacterial community at the genus level in carriers (-C) and process liquid (-L) of the temperature-ramped TBR (R1A), the thermophilic TBR (R2A), and the extreme-thermophilic TBR (R2B). Sampling in reactor R1A was based on each 5 °C increment step in the gradual ramp of temperature from 55 °C to 80 °C, while sampling in reactor R2A and R2B was performed with an interval of 3–4 days throughout the operational period.

(R2B) than at 50 °C (R2A) and declined when ramping the temperature to ≥ 75 °C in R1A, which induced a shift in the relative abundance towards *Caldanaerobacter*. A distinctive difference between *Coprothermobacter* and *Caldanaerobacter* is that many of the species of *Coprothermobacter* are proteolytic, such as *C. proteolyticus* [55], whereas many species of *Caldanaerobacter* are saccharolytic, such as *C. subterraneus* [53]. The observed increase in abundance of *Caldanaerobacter* and decrease of *Coprothermobacter* at elevated temperatures could thus be related to, in addition to the increase in temperature per se, lower biomass production and associated protein production at higher temperatures or a higher secretion of extracellular polysaccharides, which has previously been demonstrated as a response to temperature stress [56]. *A. flavidum* has been reported to possess a temperature optimum of 58 °C with growth demonstrated up to 68 °C [57], and thus operation of the TBR at 70 °C (R2B) would be at the edge of the temperature tolerance of this microbe. Statistical analysis

demonstrated that most of the bacterial families preferred the thermophilic temperatures (50 °C) over extreme-thermophilic temperatures (70 °C), where especially *Acetomicrobiaceae* was less abundant at higher temperatures ($p < 0.25$) (Fig. A5, supplementary materials).

Interestingly, the high H_2 and CO_2 concentrations in the TBRs were conjectured to sustain autotrophic bacterial growth with homoacetogenic activity and acetate production. But despite CO_2 being the sole carbon source introduced to the TBRs, many of the genera identified in the bacterial community were identified as chemoheterotrophs, i.e. *Acetomicrobium*, *Caldanaerobacter*, and *Coprothermobacter* that harbor species known to catabolize peptides and carbohydrates [57]. However, some of the genera in these families have previously been reported capable of autotrophic homoacetogenic activity such as *Acetomicrobium* [58], rendering it challenging to differentiate between autotrophic and heterotrophic acetate production. A Principal Coordinate Analysis (PCoA) was thus generated to identify correlations between the

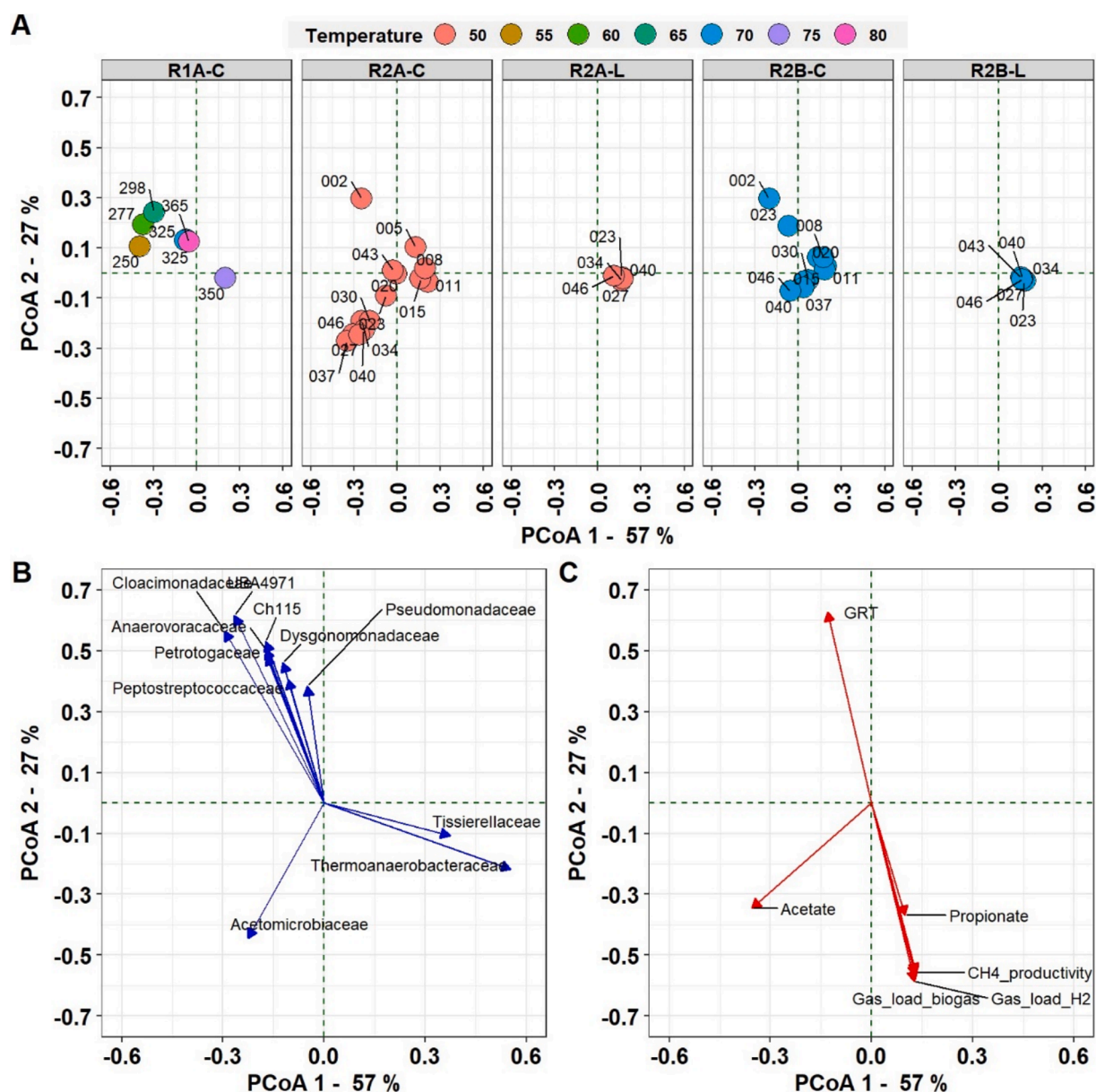


Fig. 4. Principal Coordinate analysis (PCoA) of the bacterial community relating the functional *Bacteria* to the environmental variables in the different reactors (R1A, R2A, and R2B) for both in the liquid (–L) and on the carriers (–C). A) Weighted PCoA with Unifrac distances for a subset of bacterial ASVs. B) Families qualified the permutational multiple regression significance ($p < 0.05$) among the top 20 bacterial families. C) Anaerobic digestion process parameters and volatile fatty acid results qualified the significance ($p < 0.05$) of the permutational multiple regression test. Plot B and C elucidate the multidimensional dispersion of samples visualized in two-dimensional space, where coordinates 1 and 2 (PCoA 1 and PCoA 2) explain 57 % and 27 % of the variance, respectively.

microbial structure and the process parameter (Fig. 4).

The PCoA analysis indicated that – independent of the temperature – the microbial structure in the liquid was less prone to dynamic changes from the environmental variables such as varying the H₂/CO₂ gas load or organic acids, compared with the microbial culture embedded in the carrier materials (Fig. 4A and A6). This independence indicated that the H₂/CO₂ dependent activity occurred primarily from the microbial culture immobilized on the carriers. The PCoA analysis also demonstrated that *Acetomicrobiaceae* was the primary *Bacteria* that was associated with the increasing acetate concentrations in the TBRs (Fig. 4B and 4C). The relative abundance of *Acetomicrobiaceae* became especially apparent at higher H₂/CO₂ gas loads when the CO₂ load was 10.1 L_{CO2} L_R⁻¹ d⁻¹ in R1A and had reached 13.6 L_{CO2} L_R⁻¹ d⁻¹ in R2A and 20.7 L_{CO2} L_R⁻¹ d⁻¹ in R2B. Conversely, the acetate concentration demonstrated a clear negative correlation with the bacterial families *Thermoanaerobacteraceae* and *Tissierellaceae*, which contain characterized syntrophic acetate oxidizing *Bacteria* (SAOB) [24]. The negative correlation between these families and acetate concentration suggested a continuous syntrophic acetate oxidation (SAO) activity by converting it into H₂ and CO₂. Usually, in a marginal energy economy, such as anaerobic digestion, acetate, propionate, and butyrate would be degraded by syntrophic *Bacteria* in cooperation with HMs, which would require low H₂ partial pressures. However, the high H₂ loading and associated partial pressure in the biomethanation reactors render the SAO bioenergetically unfavourable, but multiple studies have reported SAOB activity despite presumably high H₂/CO₂ concentrations [59,60]. The observation of potential SAOBs in TBRs for biomethanation could be closely linked to the macro- and micro-gradients within the TBRs. The H₂ partial pressure has been demonstrated to decline rapidly along the vertical axis of TBRs, which stratifies the reactor bed with different local environments [22], and gradient studies within methanogenic biofilms have demonstrated that the H₂ penetration into the biofilm is narrow (<0.5 mm) due to rapid H₂ consumption [61,62]. Accordingly, these gradients create suitable environments for SAO activity, and the natural presence of SAOBs thus propose an alternative strategy for acetate control by augmentation with *Bacteria* facilitating the SAO pathway in the TBRs.

3.2.2. Links between process performance and methanogenic abundance at gradually increasing temperatures

The performance and process variables of R1A were monitored continuously during the evaluation of a gradual temperature ramping period from a temperature of 55 °C to 85 °C, based on parameters such as CH₄ productivity, acetate, VFA concentration, and microbial abundance of the dominating methanogenic group *Methanobacteriales* (Fig. 5).

It was demonstrated that the CH₄ productivity could be maintained at > 10 L_{CH4} L_R⁻¹ d⁻¹ in the temperature range of 55 °C to 70 °C. At temperatures > 70 °C, the CH₄ productivity gradually decreased and ultimately diminished to 0.56 ± 0.34 L_{CH4} L_R⁻¹ d⁻¹ at 85 °C, indicating the upper-temperature limit for the HMs. Accordingly, the 16S rRNA gene copy number of the dominant methanogen order, *Methanobacteriales* (Figs. 2 and 5), correlated with a peak at 65 °C with 1.3x10⁸ copies g_{carrier}⁻¹ followed by a decline whilst ramping the temperature. Regardless of the decrease in the abundance of *Methanobacteriales* near the TBR's gas inlet region (Fig. 5B), the overall CH₄ productivity was maintained at 70 °C. (Fig. 5A). It has previously been demonstrated that the exothermic biomethanation process generates substantial amounts of heat that lead to temperature gradients within the reactor core without thermal management [6]. The demonstration of the thermostability of *Methanothermobacter*, which thrives in a broad temperature range from 55 °C to 70 °C, thus offers an advantage when designing and scaling a robust TBR system. Interestingly, the acetate concentration declined with the temperature ramp-up, suggesting that the acetate-producing microorganisms were less temperature-resistant. Increasing the temperature from 55 °C to 70 °C induced a 38 % decline in total VFA (excluding acetate), and a 62 % decline in the acetate concentration,

which correlated with the demonstrated microbial response of reduced relative abundance of *Acetomicrobium*. Only a few bioengineering studies have looked into this influence of temperature on the competition between bacteria with acetogenic functions and methanogens [11,12,20]. However, the gradual increase of temperature in TBR R1A demonstrated that the H₂ and CO₂ competition between the HMs and *Bacteria* with acetogenic-producing functions can be regulated to favor HMs. Although promising, these observations were based on a highly enriched culture, which had operated continuously for 594 days and was thus already adapted from the diverse microbial structure from the inoculum to biomethanation at thermophilic temperatures of 55 °C.

3.2.3. Thermophilic (50 °C) and extreme-thermophilic (70 °C) biomethanation

To accurately assess the effect of elevated temperatures on community development and bioreactor performance, a comparative analysis featuring two TBRs at 50 °C (R2A) and 70 °C (R2B) inoculated with fresh inoculum from a mixed thermophilic anaerobic digestion sludge was commenced and operated for 50 days. The substrate gas load was stepwise increased until the CH₄ productivity for R2A reached a plateau at a maximum CH₄ productivity of 16.86 ± 0.22 L_{CH4} L_R⁻¹ d⁻¹ on day 21–23 and 33–42. On day 24–32 and 43–50, the performance of R2A was increased even further with a gas load equivalent to 19.21 L_{CH4} L_R⁻¹ d⁻¹ at full conversion. However, despite multiple attempts, this CH₄ productivity could not be maintained and thus resulted in unconverted substrate gas deteriorating the CH₄ product gas quality (Fig. 6A). The 70 °C TBR, R2B, reached a similar plateau of a maximum CH₄ productivity of 21.01 ± 0.95 L_{CH4} L_R⁻¹ d⁻¹ on day 21–23 and 46–50, while increasing the gas load further to an equivalent of 24.02 L_{CH4} L_R⁻¹ d⁻¹ at full conversion led to instability and unconverted substrate gas in the product in the last hours before daily trickling on day 24–45. A 24.6 % increase in the maximum CH₄ productivity was recorded when comparing R2B at 70 °C to R2A at the lower 50 °C temperature. The CH₄ productivity of the 50 °C TBR correlated well with a previous study, demonstrating a CH₄ productivity of 15.4 L_{CH4} L_R⁻¹ d⁻¹ in a thermophilic TBR [7]. Additionally, a study of batch-based biomethanation assays demonstrated accordingly that increasing the temperature from 55 °C to 70 °C would enhance CH₄ productivity [54].

The lowest gas retention times of 13.9 min for the thermophilic TBR (R2A) and 10.8 min for the extreme-thermophilic TBR (R2B) (Fig. 6B) were calculated based on the gas flow inputs to the reactors. The VFA concentration grew steadily for both of the TBRs (Fig. 6C) accompanied by a transient decline in pH from day 1–12 (Fig. 6F). Acetate constituted the dominant VFA in the thermophilic TBR from day 1–9 (70.3 % acetate of the total VFA) and in the extreme-thermophilic TBR from day 1–4 (60.8 % of the total VFA) at day 2. The acetate to total VFA ratio decreased rapidly in the initial 12 days due to the accumulation of longer-chained VFAs. By day 13, the acetate to total VFA ratio stabilized for both reactors, where the acetate comprised an average of 30.3 % ± 3.6 % and 19.8 % ± 4.2 % of the total VFA in the thermophilic and extreme-thermophilic TBR for day 13–50, respectively (Fig. 6D). The acetate concentrations were in general higher at thermophilic conditions, whereas the total VFA concentration was higher for the extreme-thermophilic TBR. Although not statistically significant, a lower acetate concentration was in general demonstrated for the extreme-thermophilic TBR compared to thermophilic TBR (Fig. 6C). In addition to acetate, the longer-chained VFAs were primarily propionate and butyrate, which would be products of the mineralization of microbial biomass by chemoheterotrophic bacteria. Several studies have reported the accumulation of these VFAs at increasing gas loads due to the thermodynamic constraints of high H₂ partial pressures rendering their further degradation endergonic [7,22]. The extreme-thermophilic TBR had a 24.6 % higher turnover of CO₂ and H₂, which was expected to lead to higher biomass production compared to the thermophilic TBR, which constituted an organic carbon source for heterotrophic acidogens producing butyrate, propionate, and acetate. Accordingly, bioreactor

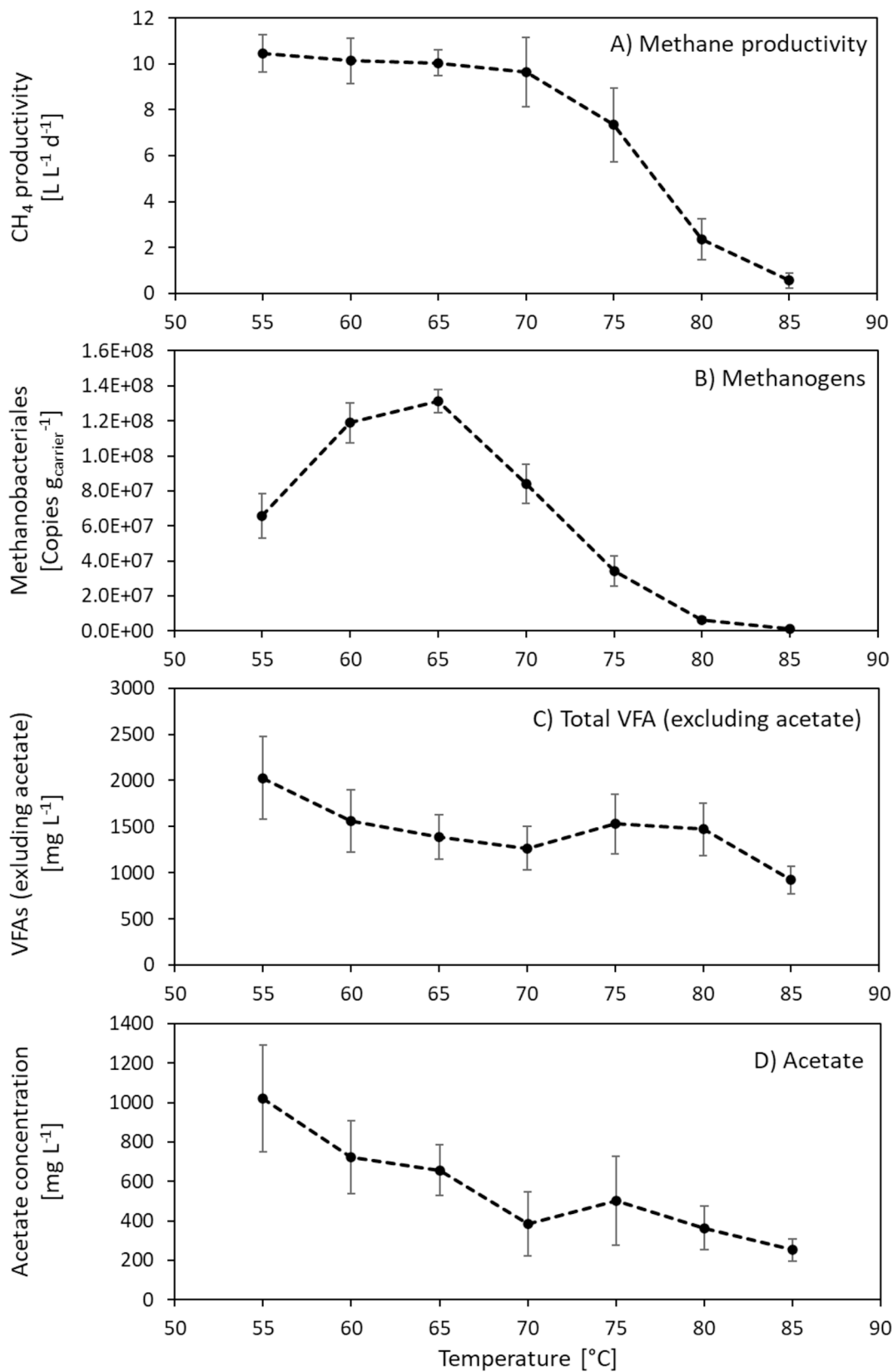


Fig. 5. Effect of gradual temperature ramping in a thermophilic TBR after two years of operation on A) CH₄ productivity, B) *Methanobacteriales* gene copies, C) total VFA, and D) acetate concentration. Different durations of the operation periods were applied at 55 °C (79 days), 60 °C (26 days), 65 °C (20 days), 70 °C (26 days), 75 °C (24 days), 80 °C (14 days), and 85 °C (6 days).

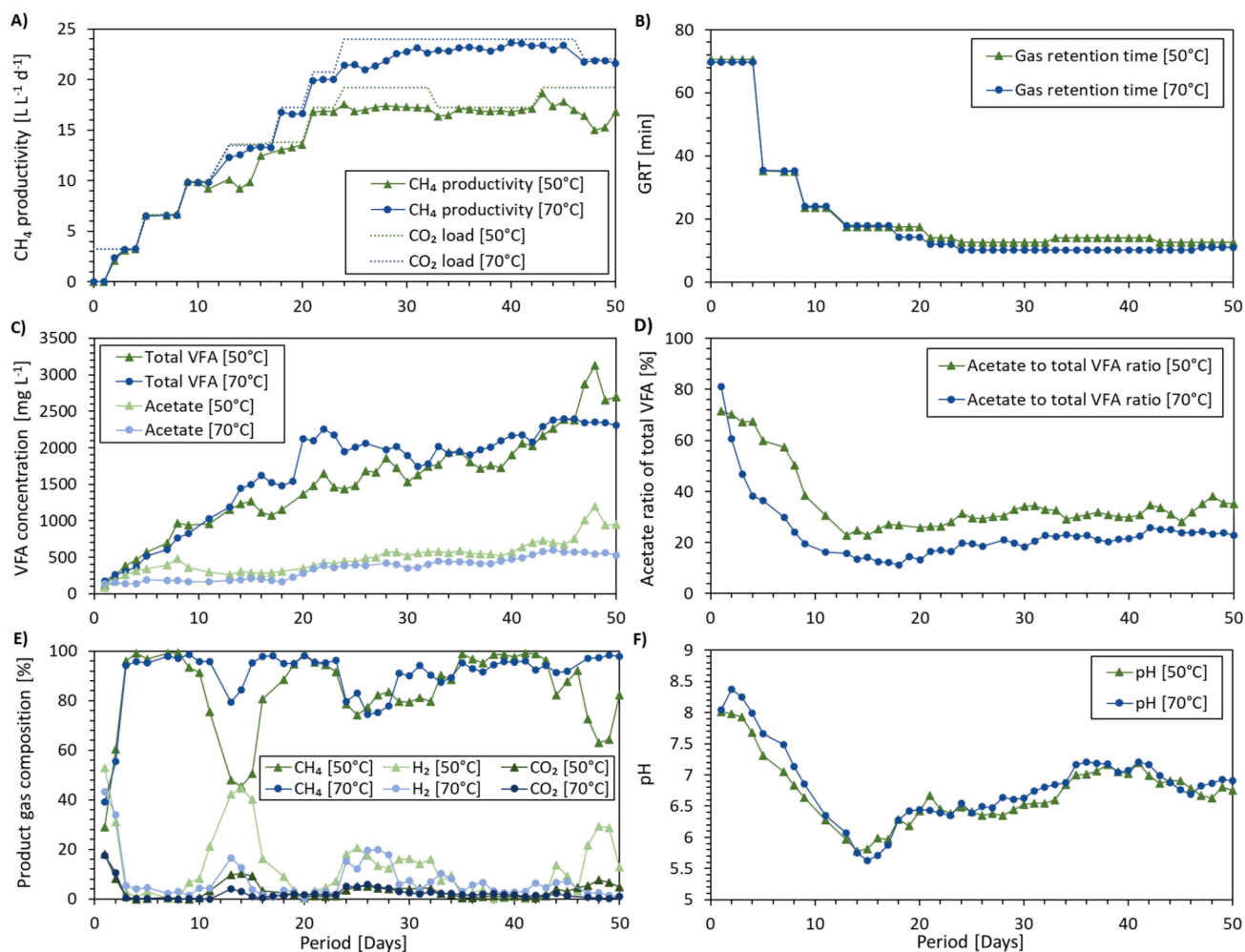


Fig. 6. Process performance parameters of a 50 °C thermophilic TBR and a 70 °C extreme-thermophilic TBR for an operation period of 50 days in regard to the A) CH₄ productivity and CO₂ gas load, B) gas retention time, C) total VFA and acetate concentrations, D) acetate to total VFA ratio, E) product gas composition, and F) pH.

studies have demonstrated that the CO₂ and H₂ assimilated into methanogenic cell material provide a continuously replenishing carbon source for heterotrophic growth, which enables nutrient recycling but leads to VFA production [23,63].

3.3. Physicochemical factors affected by process temperature in trickle bed reactors

The demonstration of notably enhancing the CH₄ productivity by 24.6 % when elevating the process temperature from 50 °C to 70 °C could be attributed to a combination of biological and physicochemical factors, of which the individual contributions remain to be elucidated. Here, the effect of temperature on the H₂ gas–liquid mass transfer rate will be modeled by examining the temperature effect on the physicochemical factors, i.e. liquid viscosity, gaseous water vapor content, gas solubility, and gas diffusion. Throughout this discussion, the H₂ mass transfer driving force is referred to as $(C^* - C_L)$. Increasing the temperature results in an increased water vapor content (by water evaporation) in the gas phase TBR. According to the Antoine equation, the water vapor content in the gas phase increases exponentially with a rise in temperature towards the boiling point of water. At 50 °C, the water vapor content corresponds to a partial pressure of 0.12 bar, but by increasing the temperature to 70 °C, the water vapor content increases to 0.31 bar. According to Dalton's law, the total pressure (in these TBRs: ambient pressure) is the sum of the partial pressures of the individual gas

components, and the partial pressure of H₂ determining the H₂ solubility (and driving force) will thus decrease due to the higher water vapor content. A further detrimental effect of the water vapor content is a reduction in GRT, which in TBRs is controllable by the ratio of the gas inflow rate and the reactor volume. The more pronounced phase transition inside of the TBR of liquid water to water vapor due to the higher temperatures forces the gaseous reactants of H₂ and CO₂ and the product of CH₄ out of the reactor bed. Both of these factors affect the TBR performance by reducing the mass transfer driving force and the GRT by 21.4 % when increasing the temperature from 50 °C to 70 °C (assuming a mass transfer limited process with C_L equal to zero). Note that although the water vapor effect directly implicates non-pressurized systems, it becomes insignificant when pressurization of the bioreactor is applied to increase the H₂ driving force (Dalton's law) since the contribution of the water vapor pressure remains the same irrespective of the total pressure. In addition to the aforementioned temperature effects on the H₂ gas–liquid driving force, the substrate source will also impact the H₂ gas–liquid mass transfer rate. The bioreactor systems relied on the supply of raw biogas for the CO₂ source, which introduced a considerable quantity of CH₄ that reduces the gas retention time and the H₂ driving force.

Furthermore, the solubility of H₂ (Henry's constant) decreases as the temperature increases, according to a model fit on experimental data in [39]. Increasing the temperature in the bioreactor from 50 °C to 70 °C reduces the dissolved gas concentration at the gas–liquid interface (C^*)

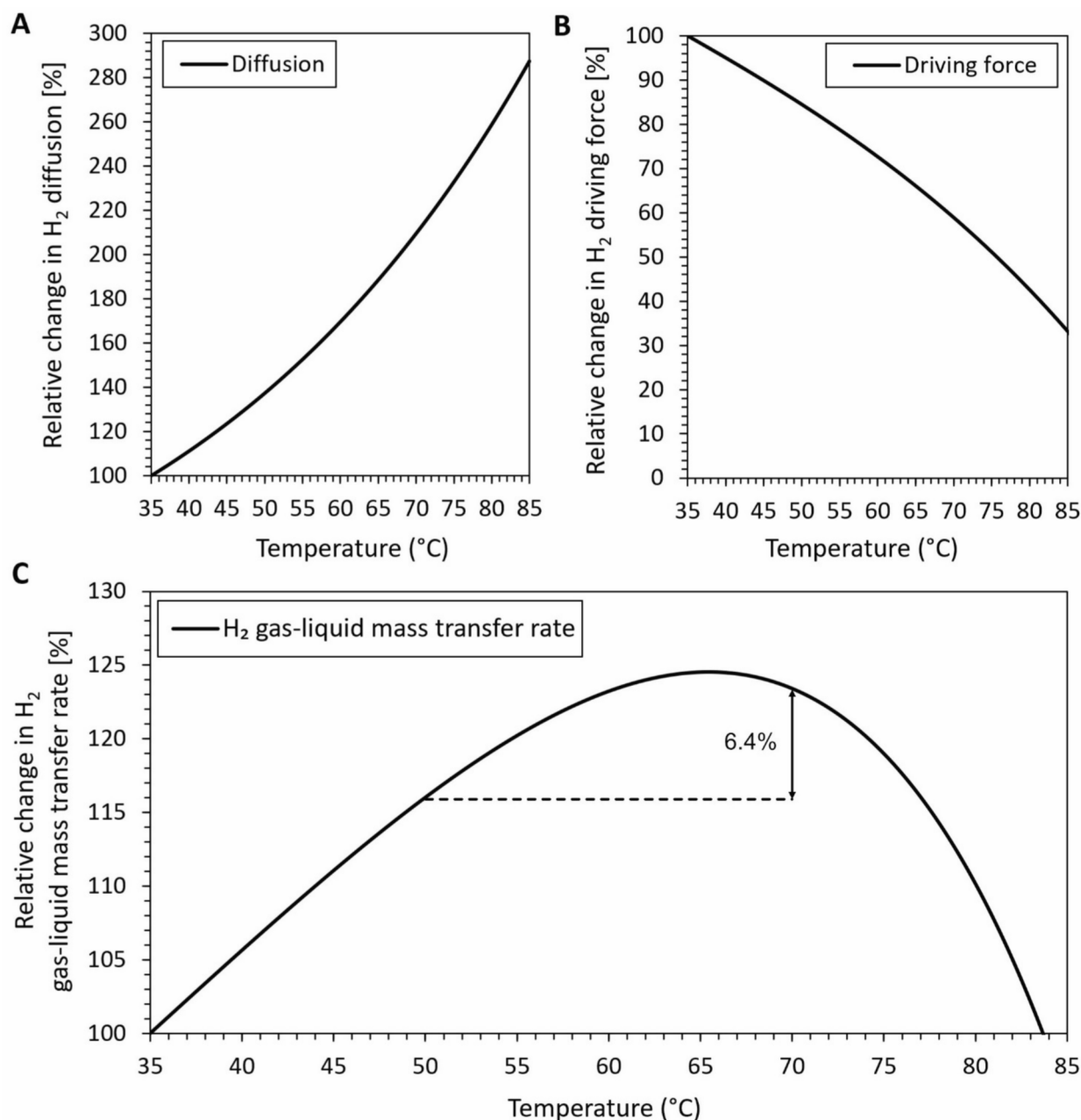


Fig. 7. The temperature-related physicochemical effects in TBRs for biomethanation at ambient pressure, i.e. lower H₂ solubility and liquid viscosity and higher H₂ diffusion rates and water vapor content at elevated temperatures. Here, the relative change in (A) the H₂ diffusion rate (proportional to k_L), (B) the H₂ driving force ($C^* - C_L$), and (C) the resultant H₂ gas-liquid mass transfer rate (r_{g-l}) compared to mesophilic temperature (35 °C) as reference (100 %). Adopted and modified from [14].

by 11.3 %. In previously reported work, increasing the temperature has been noted to induce a negative effect on the overall H₂ gas-liquid mass transfer rate, which was indirectly compensated for by higher biological activity that reduced the concentration of dissolved H₂ and hereby increased the concentration-dependent driving force [13]. However, this would imply that the system is more prone to being biologically limited rather than the general understanding of H₂ mass transfer limitation. In contrast, an analysis by Jensen et al. revealed that the increase in diffusivity exceeded the decline in driving force due to the lower solubility (Henry's constant) [14]. Based on the correlation of Akgerman and Gainer, the H₂ gas-liquid diffusivity in water increases with temperature (Fig. 7A), and is quantified as much as a 52.6 % increase when changing the temperature from 50 °C to 70 °C. With the reduced driving force that is significant at the higher temperatures (Fig. 7B), the relative

improvement in the H₂ gas-liquid mass transfer rate from temperature was calculated (Fig. 7C). For this calculation by the equation $r_{g-l} = k_L \cdot a \cdot (C^* - C_L)$, the mass transfer coefficient (k_L) has a proportional relationship to the H₂ diffusion coefficient in water, while assuming the diffusional length would remain constant [41]. However, this would be an approximation, since the diffusional length would not be entirely constant during steady-state due to physical properties such as the liquid viscosity [64], which decreases at higher temperatures leading to a shorter static liquid hold-up (i.e. diffusional length) and thus an enhanced H₂ gas-liquid mass transfer rate. The effect of temperature on the interfacial area, a , is a function of biological and physicochemical factors. Biologically, it is influenced by the methanogenic biofilm coverage on the heterogenous carriers, while physicochemically, it is influenced by the extent of the stagnant water film covering the biofilm.

The methanogenic biofilm development on carrier materials in biomethanation remains an active field of research [65,66] and a direct relationship with temperature remains to be established. Physical parameters such as the water surface tension will be temperature-dependent and drops by 3.9 % from 55 °C to 70 °C [67], which influences the extent of the stagnant water layer and the droplet generation in the TBR. However, the stagnant water layer will rely on both carrier geometry, surface hydrophilicity, and bridging effects between the individual carriers. Consequently, while the effect of temperature on the gas–liquid interfacial area of packed bed carrier materials is complex to quantify, due to capillary phenomena such as liquid bridging between the carriers, it is expected to be minimal and largely independent of the temperature [68], and is here treated as a constant. While this approximation would be valid for TBRs, it would not be for CSTRs and other bubble dispersion bioreactors relying on bubble formation and dispersion. Additionally, if the system is H₂ mass transfer limited, the concentration of H₂ in the bulk liquid (C_L) can be set to zero.

By combining all these thermodynamic effects on the H₂ gas–liquid mass transfer rate (Fig. 7C), it is demonstrated that increasing the temperature from mesophilic conditions up to 65.4 °C would improve the gas–liquid mass transfer rate of H₂. However, above 65.4 °C the mass transfer rate would decrease due to the overwhelming contribution of the reduced H₂ mass transfer driving force (Fig. 7B) and the immanent effects of the water vapor content. This determination is an expansion of the H₂ mass transfer dynamic (with temperature) presented by Jensen et al., who only considered the solubility of H₂ in the driving force estimation, and neglected the contributions of varying water vapor content on the H₂ partial pressure [14]. It should also be noted that applying other diffusion and mass transfer models could alter the relative changes in the overall gas–liquid mass transfer rate of H₂.

The implications of increasing the temperature from 50 °C to 70 °C in this study would, according to the H₂ gas–liquid mass transfer rate (Fig. 7C), bring an improvement of 6.4 % in the mass transfer rate (and equally in the CH₄ productivity if mass transfer limitation is assumed). This improvement remains far below the 24.6 % improvement in CH₄ productivity achieved experimentally in the study, which indicates the presence of a clear biological enhancement factor by increasing the TBR temperature. This tendency of improved conversion rates due to microbial factors has previously been demonstrated in mass transfer-limited systems [69]. The biological enhancement factor is considered as the extent of reaction in the stagnant liquid film diffusion layer based on the Hatta number, which depends on the specific microbial activity, the biomass concentration, the cell distribution profile in the stagnant liquid layer covering the biofilm, the gas diffusion coefficient in the liquid, and the driving force [14,70]. The observed enhancement in the CH₄ productivity – beyond the 6.4 % contribution in improvement by the H₂ gas–liquid mass transfer rate – when increasing the temperature from 50 °C to 70 °C indicates a significant improvement in the biological enhancement factor as a result of the increase in the biological H₂ consumption rate that contributes significantly more than the theoretical increase in the H₂ transfer rate. The higher conversion rates achievable at higher temperatures should thus encourage further in-depth research to explore the temperature regimes of >50 °C including the utilization of hyperthermophilic HMs for biomethanation to promote the biological enhancement factor even further.

4. Conclusion

The temperature of the biomethanation process has proven to have intricate effects on the biological community and the thermodynamics governing TBR biomethanation. The presented work demonstrated recurring acidification of a long-term enriched TBR, R1A. Multiple strategies were tested to alleviate the VFA accumulation, but most of these techniques were based on liquid trickling, which was found to reduce the CH₄ productivity transiently. The effect of utilizing temperature as a pinch parameter towards methanogenesis was subsequently

examined. Ramping the temperature from 55 °C to 70 °C demonstrated a reduction in the acetate concentration by 62 %. Nevertheless, further increments in temperature above 70 °C reduced the methanogenic conversion and proliferation of *Methanobacteriales*, the dominating HM; at 85 °C the methanogenic activity was eliminated. A comparative analysis of two TBRs (respectively R2A and R2B) operated at thermophilic (50 °C) and extreme-thermophilic (70 °C) conditions demonstrated a 24.6 % improvement in CH₄ productivity as a response to favored extreme-thermophilic temperature. To understand this improvement, the H₂ gas–liquid mass transfer rate was modeled and demonstrated a 6.4 % improvement at 70 °C (vs 50 °C). The contribution of biological factors to the enhancement in CH₄ productivity is credited for the performance improvement, regardless of the H₂ gas–liquid mass transfer rate being considered the rate-limiting barrier in biomethanation. Ultimately, this work provides new knowledge on biological communities and process factors that improve the competitiveness of TBR biomethanation as a technology for CO₂ and H₂ conversion into carbon-based chemical energy carriers.

CRedit authorship contribution statement

Mads Ujark Sieborg: Writing – original draft, Visualization, Methodology, Investigation, Formal analysis, Data curation, Conceptualization. **Nicolaas Engelbrecht:** Writing – review & editing, Investigation, Formal analysis, Data curation. **Abhijeet Singh:** Writing – review & editing, Visualization, Formal analysis, Data curation. **Anna Schnürer:** Writing – review & editing, Supervision, Resources, Methodology, Funding acquisition, Conceptualization. **Lars Ditlev Mørck Ottosen:** Writing – review & editing, Resources, Methodology, Funding acquisition, Conceptualization. **Michael Vedel Wegener Kofoed:** Writing – review & editing, Supervision, Resources, Project administration, Funding acquisition, Conceptualization.

Funding

This work was funded by (1) Apple Inc. as part of the APPLAUSE bioenergy collaboration with Aarhus University, (2) SLU and (3) Research council VR (2021-04891).

Declaration of competing interest

The authors declare the following financial interests/personal relationships which may be considered as potential competing interests: [Mads Ujark Sieborg, Nicolaas Engelbrecht reports financial support was provided by Apple Inc. If there are other authors, they declare that they have no known competing financial interests or personal relationships that could have appeared to influence the work reported in this paper].

Acknowledgements

The authors would like to thank Simon Isaksson and Maria Victoria Goddio from the Swedish University of Agricultural Sciences for their technical support.

Appendix A. Supplementary material

Supplementary data to this article can be found online at <https://doi.org/10.1016/j.cej.2025.161179>.

Data availability

Data will be made available on request.

References

- [1] J. Rogelj, D. Shindell, K. Jiang, S. Fifita, P. Forster, V. Ginzburg, C. Handa, H. Kheshgi, S. Kobayashi, E. Kriegler, L. Mundaca, R. Séférián, M.V. Vilarino, Mitigation Pathways Compatible with 1.5°C in the Context of Sustainable Development, in: V. Masson-Demotte, P. Zhai, H.-O. Pörtner, D. Roberts, J. Skea, P. R. Shukla, A. Pirani, W. Moufouma-Okia, C. Péan, R. Pidcock, S. Connors, J.B.R. Matthews, Y. Chen, X. Zhou, M.I. Gomis, E. Lonnoy, T. Maycock, M. Tignor, T. Waterfield (Eds.), *Glob. Warm. 1.5°C. An IPCC Spec. Rep. Impacts Glob. Warm. 1.5°C above Pre-Industrial Levels Relat. Glob. Greenh. Gas Emiss. Pathways, Context Strength. Glob. Response to Threat Clim. Chang.*, 2018.
- [2] IEA, *Renewables 2022*, 2022. <https://www.iea.org/reports/renewables-2022>.
- [3] M. Burkhardt, G. Busch, Methanation of hydrogen and carbon dioxide, *Appl. Energy*. 111 (2013) 74–79, <https://doi.org/10.1016/j.apenergy.2013.04.080>.
- [4] N. Nishimura, S. Kitaura, A. Mimura, Y. Takahara, Cultivation of thermophilic methanogen KN-15 on H₂-CO₂ under pressurized conditions, *J. Ferment. Bioeng.* 73 (1992) 477–480, [https://doi.org/10.1016/0922-338X\(92\)90141-G](https://doi.org/10.1016/0922-338X(92)90141-G).
- [5] N. Nishimura, S. Kitaura, A. Mimura, Y. Takahara, Growth of thermophilic methanogen KN-15 on H₂-CO₂ under batch and continuous conditions, *J. Ferment. Bioeng.* 72 (1991) 280–284, [https://doi.org/10.1016/0922-338X\(91\)90164-C](https://doi.org/10.1016/0922-338X(91)90164-C).
- [6] N. Engelbrecht, M.U. Sieborg, L.D.M. Ottosen, M.V.W. Kofoed, Metabolic heat production impacts industrial upscaling of ex situ biomethanation trickle-bed reactors, *Energy Convers. Manag.* 299 (2024) 117769, <https://doi.org/10.1016/j.enconman.2023.117769>.
- [7] D. Strübing, B. Huber, M. Lebuhn, J.E. Drewes, K. Koch, High performance biological methanation in a thermophilic anaerobic trickle bed reactor, *Bioresour. Technol.* 245 (2017) 1176–1183, <https://doi.org/10.1016/j.biortech.2017.08.088>.
- [8] P. Noll, L. Lilje, R. Hausmann, M. Henkel, Modeling and exploiting microbial temperature response, *Processes*. 8 (2020), <https://doi.org/10.3390/pr8010121>.
- [9] T.M. Hoehler, Biological energy requirements as quantitative boundary conditions for life in the subsurface, *Geobiology* 2 (2004) 205–215, <https://doi.org/10.1111/j.1472-4677.2004.00033.x>.
- [10] B.M. Zeldes, M.W. Keller, A.J. Loder, C.T. Straub, M.W.W. Adams, R.M. Kelly, Extremely thermophilic microorganisms as metabolic engineering platforms for production of fuels and industrial chemicals, *Front. Microbiol.* 6 (2015) 1–17, <https://doi.org/10.3389/fmicb.2015.01209>.
- [11] K. Asimakopoulou, M. Łęz, A. Grimalt-alemany, A. Melas, Z. Wen, H.N. Gavala, I. V. Skiadas, Temperature effects on syngas biomethanation performed in a trickle bed reactor, *Chem. Eng. J.* 393 (2020) 124739, <https://doi.org/10.1016/j.cej.2020.124739>.
- [12] A. Lemmer, T. Ullrich, Effect of different operating temperatures on the biological hydrogen methanation in trickle bed reactors, *Energies* 11 (2018) 1344, <https://doi.org/10.3390/en11061344>.
- [13] B. Lecker, L. Illi, A. Lemmer, H. Oechsner, Biological hydrogen methanation – A review, *Bioresour. Technol.* 245 (2017) 1220–1228, <https://doi.org/10.1016/j.biortech.2017.08.176>.
- [14] M.B. Jensen, L.D.M. Ottosen, M.V.W. Kofoed, H₂ gas-liquid mass transfer: a key element in biological power-to-gas methanation, *Renew. Sustain. Energy Rev.* 147 (2021) 111209, <https://doi.org/10.1016/j.rser.2021.111209>.
- [15] N.J.R. Kraakman, J. Rocha-Rios, M.C.M. Van Loosdrecht, Review of mass transfer aspects for biological gas treatment, *Appl. Microbiol. Biotechnol.* 91 (2011) 873–886, <https://doi.org/10.1007/s00253-011-3365-5>.
- [16] D.L. Valentine, Adaptations to energy stress dictate the ecology and evolution of the Archaea, *Nat. Rev. Microbiol.* 5 (2007) 316–323, <https://doi.org/10.1038/nrmicro1619>.
- [17] B. Jiang, X. Hu, U. Söderlind, K. Göransson, W. Zhang, C. Yu, Identification of the biometanation pathways during biological CO₂ fixation with exogenous H₂ addition, *Fuel Process. Technol.* 238 (2022) 107478, <https://doi.org/10.1016/j.fuproc.2022.107478>.
- [18] L. Chen, S. Du, L. Xie, Effects of pH on ex-situ biometanation with hydrogenotrophic methanogens under thermophilic and extreme-thermophilic conditions, *J. Biosci. Bioeng.* 131 (2021) 168–175, <https://doi.org/10.1016/j.jbiosc.2020.09.018>.
- [19] B.K. Ahring, A.A. Ibrahim, Z. Mladenovska, Effect of temperature increase from 55 to 65°C on performance and microbial population dynamics of an anaerobic reactor treating cattle manure, *Water Res.* 35 (2001) 2446–2452, [https://doi.org/10.1016/S0043-1354\(00\)00526-1](https://doi.org/10.1016/S0043-1354(00)00526-1).
- [20] D. Andreides, D. Stransky, J. Bartackova, D. Pokorna, J. Zabranska, Syngas biometanation in countercurrent flow trickle-bed reactor operated under different temperature conditions, *Renew. Energy*. 199 (2022) 1329–1335, <https://doi.org/10.1016/j.renene.2022.09.072>.
- [21] N. Figeac, E. Trably, N. Bernet, J.P. Delgenès, R. Escudé, Temperature and inoculum origin influence the performance of ex-situ biological hydrogen methanation, *Molecules* 25 (2020), <https://doi.org/10.3390/molecules25235665>.
- [22] M.U. Sieborg, L.D.M. Ottosen, M.V.W. Kofoed, Enhanced process control of trickle-bed reactors for biometanation by vertical profiling directed by hydrogen microsensor monitoring, *Bioresour. Technol.* 384 (2023) 129242, <https://doi.org/10.1016/j.biortech.2023.129242>.
- [23] M.U. Sieborg, N. Engelbrecht, L.D.M. Ottosen, M.V.W. Kofoed, Sunshine-to-fuel: Demonstration of coupled photovoltaic-driven biometanation operation, process, and techno-economical evaluation, *Energy Convers. Manag.* 299 (2024) 117767, <https://doi.org/10.1016/j.enconman.2023.117767>.
- [24] B. Müller, L. Sun, M. Westerholm, A. Schnürer, Bacterial community composition and fhs profiles of low- and high-ammonia biogas digesters reveal novel syntrophic acetate-oxidising bacteria, *Biotechnol. Biofuels*. 9 (2016) 1–18, <https://doi.org/10.1186/s13068-016-0454-9>.
- [25] L.W. Hugerth, H.A. Wefer, S. Lundin, H.E. Jakobsson, M. Lindberg, S. Rodin, L. Engstrand, A.F. Andersson, DegePrime, a program for degenerate primer design for broad-taxonomic-range PCR in microbial ecology studies, *Appl. Environ. Microbiol.* 80 (2014) 5116–5123, <https://doi.org/10.1128/AEM.01403-14>.
- [26] M. Martín, Cutadapt removes adapter sequences from high-throughput sequencing reads, *EMBnet J.* 17 (2011) 10–12, <https://doi.org/10.14806/ej.17.1.200>.
- [27] T. Rognes, T. Flouri, B. Nichols, C. Quince, F. Mahé, VSEARCH: A versatile open source tool for metagenomics, *PeerJ* 4 (2016), <https://doi.org/10.7717/peerj.2584>.
- [28] B.J. Callahan, P.J. McMurdie, M.J. Rosen, A.W. Han, A.J.A. Johnson, S.P. Holmes, DADA2: High-resolution sample inference from Illumina amplicon data, *Nat. Methods*. 13 (2016) 581–583, <https://doi.org/10.1038/nmeth.3869>.
- [29] RStudio Team, RStudio: Integrated Development Environment for R, (2020). <http://www.rstudio.com>.
- [30] R Core Team, R: A language and environment for statistical computing, (2021). <https://www.r-project.org/>.
- [31] A. Alishum, DADA2 formatted 16S rRNA gene sequences for both bacteria & archaea, (2021). doi: 10.5281/zenodo.4735821.
- [32] P.J. McMurdie, S. Holmes, Phyloseq: an R package for reproducible interactive analysis and graphics of microbiome census data, *PLoS One* 8 (2013) 1–11, <https://doi.org/10.1371/journal.pone.0061217>.
- [33] J. Oksanen, G.L. Simpson, F.G. Blanchet, R. Kindt, P. Legendre, P.R. Minchin, R. B. O'Hara, P. Solyms, M.H.H. Stevens, Vegan: community ecology package, *Compr. R Arch. Netw.* (2019).
- [34] H. Wickham, Data Analysis, in: *Ggplot2 Elegant Graphs*, Springer International Publishing, Cham, 2016, pp. 189–201, https://doi.org/10.1007/978-3-319-24277-4_9.
- [35] M.I. Love, W. Huber, S. Anders, Moderated estimation of fold change and dispersion for RNA-seq data with DESeq2, *Genome Biol.* 15 (2014) 1–21, <https://doi.org/10.1186/s13059-014-0550-8>.
- [36] T. Narihiro, Y. Sekiguchi, Oligonucleotide primers, probes and molecular methods for the environmental monitoring of methanogenic archaea, *Microb. Biotechnol.* 4 (2011) 585–602, <https://doi.org/10.1111/j.1751-7915.2010.00239.x>.
- [37] R.H. Perry, D.W. Green, Perry's Chemical Engineers' Handbook, 8th Edition, 2013. doi: 10.1017/CBO9781107415324.004.
- [38] Grischuk, Archiv für Energiewirtschaft, 11 (1957).
- [39] N.I. Kolev, Solubility of O₂, N₂, H₂ and CO₂ in water, in: N.I. Kolev (Ed.), *Multiph. Flow Dyn.*, 4, Springer Berlin Heidelberg, Berlin, Heidelberg, 2011, pp. 209–239, https://doi.org/10.1007/978-3-642-20749-5_11.
- [40] R. Sander, Compilation of Henry's law constants (version 4.0) for water as solvent, *Atmos. Chem. Phys.* 15 (2015) 4399–4981, <https://doi.org/10.5194/acp-15-4399-2015>.
- [41] J.C. Charpentier, Mass-transfer rates in gas-liquid absorbers and reactors, 1981. doi: 10.1016/S0065-2377(08)60025-3.
- [42] A. Akgerman, J.L. Gainer, Predicting gas-liquid diffusivities, *J. Chem. Eng. Data*. 17 (1972) 372–377.
- [43] L. Leng, P. Yang, S. Singh, H. Zhuang, L. Xu, W.H. Chen, J. Dolfig, D. Li, Y. Zhang, H. Zeng, W. Chu, P.H. Lee, A review on the bioenergetics of anaerobic microbial metabolism close to the thermodynamic limits and its implications for digestion applications, *Bioresour. Technol.* 247 (2018) 1095–1106, <https://doi.org/10.1016/j.biortech.2017.09.103>.
- [44] P. Tsapekos, M. Alvarado-morales, I. Angelidaki, H₂ competition between homoacetogenic bacteria and methanogenic archaea during biometanation from a combined experimental-modelling approach, *J. Environ. Chem. Eng.* 10 (2022) 107281, <https://doi.org/10.1016/j.jece.2022.107281>.
- [45] T.L. Dupnock, M.A. Deshusses, Detailed investigations of dissolved hydrogen and hydrogen mass transfer in a biotrickling filter for upgrading biogas, *Bioresour. Technol.* 290 (2019) 121780, <https://doi.org/10.1016/j.biortech.2019.121780>.
- [46] A.J. Guneratnam, E. Ahern, J.A. FitzGerald, S.A. Jackson, A. Xia, A.D.W. Dobson, J. D. Murphy, Study of the performance of a thermophilic biological methanation system, *Bioresour. Technol.* 225 (2017) 308–315, <https://doi.org/10.1016/j.biortech.2016.11.066>.
- [47] M. Thema, T. Weidlich, A. Kaul, A. Böllmann, H. Huber, A. Bellack, J. Karl, M. Sterner, Optimized biological CO₂-methanation with a pure culture of thermophilic methanogenic archaea in a trickle-bed reactor, *Bioresour. Technol.* 333 (2021), <https://doi.org/10.1016/j.biortech.2021.125135>.
- [48] Electrochaea, Power-to-Gas : Electrochaea is awarded patent on super single-celled organisms for biometane production, (2017) 1–2. <https://www.electrochaea.com/latest-news/press-release-electrochaea-is-awarded-patent-on-super-single-celled-organisms-for-biomethane-production/> (accessed August 2, 2023).
- [49] K. Sasaki, M. Morita, D. Sasaki, J. Nagaoka, N. Matsumoto, N. Ohmura, H. Shinozaki, Syntrophic degradation of proteinaceous materials by the thermophilic strains *Coprothermobacter proteolyticus* and *Methanothermobacter thermautotrophicus*, *J. Biosci. Bioeng.* 112 (2011) 469–472, <https://doi.org/10.1016/j.jbiosc.2011.07.003>.
- [50] N. Lackner, A.O. Wagner, R. Markt, P. Illmer, Ph and phosphate induced shifts in carbon flow and microbial community during thermophilic anaerobic digestion, *Microorganisms*. 8 (2020), <https://doi.org/10.3390/microorganisms8020286>.
- [51] D. Kamravamesh, J.M. Rinta Kanto, H. Ali-Loytty, A. Myllärinen, M. Saalasti, J. Rintala, M. Kokko, Ex-situ biological hydrogen methanation in trickle bed reactors: Integration into biogas production facilities, *Chem. Eng. Sci.* 269 (2023) 118498, <https://doi.org/10.1016/j.ces.2023.118498>.
- [52] A. Xirostylidou, M. Gaspari, K.N. Kontogiannopoulos, G. Ghiotto, L. Treu, S. Campanaro, A.I. Zouboulis, P.G. Kougiadis, Biomethanation on demand: Continuous and intermittent hydrogen supply on biological CO₂ methanation, *Chem. Eng. J.* 495 (2024) 153677, <https://doi.org/10.1016/j.cej.2024.153677>.

- [53] M.L. Fardeau, M. Magot, B.K.C. Patel, P. Thomas, J.L. Garcia, B. Ollivier, *Thermoanaerobacter subterraneus* sp. nov., a novel thermophile isolated from oilfield water, *Int. J. Syst. Evol. Microbiol.* 50 (2000) 2141–2149, <https://doi.org/10.1099/00207713-50-6-2141>.
- [54] N. Dong, F. Bu, Q. Zhou, S.K. Khanal, L. Xie, Performance and microbial community of hydrogenotrophic methanogenesis under thermophilic and extreme-thermophilic conditions, *Bioresour. Technol.* 266 (2018) 454–462, <https://doi.org/10.1016/j.biortech.2018.05.105>.
- [55] B.M. Ollivier, R.A. Mah, T.J. Ferguson, D.R. Boone, J.L. Garcia, R. Robinson, Emendation of the genus *thermobacteroides*: *thermobacteroides proteolyticus* sp. nov., a proteolytic acetogen from a methanogenic enrichment, *Int. J. Syst. Evol. Microbiol.* 35 (1985) 425–428, <https://doi.org/10.1099/00207713-35-4-425>.
- [56] W.J. Gao, X. Qu, K.T. Leung, B.Q. Liao, Influence of temperature and temperature shock on sludge properties, cake layer structure, and membrane fouling in a submerged anaerobic membrane bioreactor, *J. Memb. Sci.* 421–422 (2012) 131–144, <https://doi.org/10.1016/j.memsci.2012.07.003>.
- [57] E. Soutschek, J. Winter, F. Schindler, O. Kandler, *Acetomicrobium flavidum*, gen. nov., sp. nov., a thermophilic, anaerobic bacterium from sewage sludge, forming acetate, CO₂ and H₂ from Glucose, *Syst. Appl. Microbiol.* 5 (1984) 377–390, [https://doi.org/10.1016/S0723-2020\(84\)80039-9](https://doi.org/10.1016/S0723-2020(84)80039-9).
- [58] J.S. Poulsen, N. de Jonge, W.V. Macêdo, F.R. Dalby, A. Feilberg, J.L. Nielsen, Characterisation of cellulose-degrading organisms in an anaerobic digester, *Bioresour. Technol.* 351 (2022) 126933, <https://doi.org/10.1016/j.biortech.2022.126933>.
- [59] I. Bassani, P.G. Kougiass, L. Treu, I. Angelidaki, Biogas upgrading via hydrogenotrophic methanogenesis in two-stage continuous stirred tank reactors at mesophilic and thermophilic conditions, *Environ. Sci. Technol.* 49 (2015) 12585–12593, <https://doi.org/10.1021/acs.est.5b03451>.
- [60] P. Ghofrani-Isfahani, P. Tsapekos, M. Peprah, P. Kougiass, A. Zervas, X. Zhu, Z. Yang, C.S. Jacobsen, I. Angelidaki, Ex-situ biogas upgrading in thermophilic trickle bed reactors packed with micro-porous packing materials, *Chemosphere* 296 (2022) 133987, <https://doi.org/10.1016/j.chemosphere.2022.133987>.
- [61] K. Maegaard, E. Garcia-Robledo, M.V.W. Kofoed, L.M. Agneessens, N. de Jonge, J. L. Nielsen, L.D.M. Ottosen, L.P. Nielsen, N.P. Revsbech, Biogas upgrading with hydrogenotrophic methanogenic biofilms, *Bioresour. Technol.* 287 (2019) 121422, <https://doi.org/10.1016/j.biortech.2019.121422>.
- [62] E. Garcia-Robledo, L.D.M. Ottosen, N.V. Voigt, M.W. Kofoed, N.P. Revsbech, Micro-scale H₂-CO₂ dynamics in a hydrogenotrophic methanogenic membrane reactor, *Front. Microbiol.* 7 (2016) 1276, <https://doi.org/10.3389/fmicb.2016.01276>.
- [63] H.K. Aghtaei, S. Püttker, I. Maus, R. Heyer, L. Huang, A. Sczyrba, U. Reichl, D. Bendorf, Adaptation of a microbial community to demand-oriented biological methanation, *Biotechnol. Biofuels Bioprod.* 15 (2022) 1–19, <https://doi.org/10.1186/s13068-022-02207-w>.
- [64] Y. Yang, Y. Xiang, G. Chu, H. Zou, Y. Luo, M. Arowo, J.F. Chen, A noninvasive X-ray technique for determination of liquid holdup in a rotating packed bed, *Chem. Eng. Sci.* 138 (2015) 244–255, <https://doi.org/10.1016/j.ces.2015.07.044>.
- [65] F. Habouzit, J. Hamelin, G. Santa-Catalina, J.P. Steyer, N. Bernet, Biofilm development during the start-up period of anaerobic biofilm reactors: The biofilm Archaea community is highly dependent on the support material, *Microb. Biotechnol.* 7 (2014) 257–264, <https://doi.org/10.1111/1751-7915.12115>.
- [66] M.B. Jensen, D. Strübing, N. de Jonge, J.L. Nielsen, L.D.M. Ottosen, K. Koch, M.V. W. Kofoed, Stick or leave – pushing methanogens to biofilm formation for ex situ biomethanation, *Bioresour. Technol.* 291 (2019) 121784, <https://doi.org/10.1016/J.BIORTECH.2019.121784>.
- [67] N.B. Vargaftik, B.N. Volkov, L.D. Voljak, International tables of the surface tension of water, *J. Phys. Chem. Ref. Data.* 12 (1983) 817–820, <https://doi.org/10.1063/1.555688>.
- [68] R.E. Tsai, A.F. Seibert, R.B. Eldridge, G.T. Rochelle, Influence of viscosity and surface tension on the effective mass transfer area of structured packing, *Energy Procedia* 1 (2009) 1197–1204, <https://doi.org/10.1016/j.egypro.2009.01.157>.
- [69] J.L. Vasel, P. Schrobiltgen, Oxygen transfer in trickling filters, *Water Res.* 25 (1991) 53–60, [https://doi.org/10.1016/0043-1354\(91\)90098-B](https://doi.org/10.1016/0043-1354(91)90098-B).
- [70] F. Garcia-Ochoa, E. Gomez, Bioreactor scale-up and oxygen transfer rate in microbial processes: an overview, *Biotechnol. Adv.* 27 (2009) 153–176, <https://doi.org/10.1016/j.biotechadv.2008.10.006>.